



# Transcriptomic, Protein-DNA Interaction, and Metabolomic Studies of VosA, VelB, and WetA in *Aspergillus nidulans* Asexual Spores

Ming-Yueh Wu,<sup>a\*</sup> Matthew E. Mead,<sup>b</sup> Mi-Kyung Lee,<sup>c</sup> George F. Neuhaus,<sup>d</sup> Donovan A. Adressa,<sup>d</sup> Julia I. Martien,<sup>a,e</sup> Ye-Eun Son,<sup>f</sup> Heungyun Moon,<sup>a</sup> Daniel Amador-Noguez,<sup>a,g</sup> Kap-Hoon Han,<sup>h</sup> Antonis Rokas,<sup>b</sup> Sandra Loesgen,<sup>d,e</sup> Jae-Hyuk Yu,<sup>a,i</sup> Hee-Soo Park<sup>f</sup>

<sup>a</sup>Department of Bacteriology, University of Wisconsin—Madison, Madison, Wisconsin, USA

<sup>b</sup>Department of Biological Sciences, Vanderbilt University, Nashville, Tennessee, USA

<sup>c</sup>Biological Resource Center (BRC), Korea Research Institute of Bioscience and Biotechnology (KRIBB), Jeongeup-si, Republic of Korea

<sup>d</sup>Department of Chemistry, Oregon State University, Corvallis, Oregon, USA

<sup>e</sup>The Whitney Laboratory for Marine Bioscience, University of Florida, Gainesville, Florida, USA

<sup>f</sup>School of Food Science and Biotechnology, Kyungpook National University, Daegu, Republic of Korea

<sup>g</sup>DOE Great Lakes Bioenergy Research Center, University of Wisconsin—Madison, Madison, Wisconsin, USA

<sup>h</sup>Department of Pharmaceutical Engineering, Woosuk University, Wanju, Republic of Korea

<sup>i</sup>Department of Systems Biotechnology, Konkuk University, Seoul, Republic of Korea

Ming-Yueh Wu and Matthew E. Mead contributed equally to this article. Author order was determined by the level of contribution in preparing the figures and the manuscript.

**ABSTRACT** In filamentous fungi, asexual development involves cellular differentiation and metabolic remodeling leading to the formation of intact asexual spores. The development of asexual spores (conidia) in *Aspergillus* is precisely coordinated by multiple transcription factors (TFs), including VosA, VelB, and WetA. Notably, these three TFs are essential for the structural and metabolic integrity, i.e., proper maturation, of conidia in the model fungus *Aspergillus nidulans*. To gain mechanistic insight into the complex regulatory and interdependent roles of these TFs in asexual sporogenesis, we carried out multi-omics studies on the transcriptome, protein-DNA interactions, and primary and secondary metabolism employing *A. nidulans* conidia. RNA sequencing and chromatin immunoprecipitation sequencing analyses have revealed that the three TFs directly or indirectly regulate the expression of genes associated with heterotrimeric G-protein signal transduction, mitogen-activated protein (MAP) kinases, spore wall formation and structural integrity, asexual development, and primary/secondary metabolism. In addition, metabolomics analyses of wild-type and individual mutant conidia indicate that these three TFs regulate a diverse array of primary metabolites, including those in the tricarboxylic acid (TCA) cycle, certain amino acids, and trehalose, and secondary metabolites such as sterigmatocystin, emericellamide, austinol, and dehydroaustinol. In summary, WetA, VosA, and VelB play interdependent, overlapping, and distinct roles in governing morphological development and primary/secondary metabolic remodeling in *Aspergillus* conidia, leading to the production of vital conidia suitable for fungal proliferation and dissemination.

**IMPORTANCE** Filamentous fungi produce a vast number of asexual spores that act as efficient propagules. Due to their infectious and/or allergenic nature, fungal spores affect our daily life. *Aspergillus* species produce asexual spores called conidia; their formation involves morphological development and metabolic changes, and the associated regulatory systems are coordinated by multiple transcription factors (TFs). To understand the underlying global regulatory programs and cellular outcomes associated with conidium formation, genomic and metabolomic analyses were performed in the model fungus *Aspergillus nidulans*. Our results show that the fungus-specific WetA/VosA/

**Citation** Wu M-Y, Mead ME, Lee M-K, Neuhaus GF, Adressa DA, Martien JI, Son Y-E, Moon H, Amador-Noguez D, Han K-H, Rokas A, Loesgen S, Yu J-H, Park H-S. 2021. Transcriptomic, protein-DNA interaction, and metabolomic studies of VosA, VelB, and WetA in *Aspergillus nidulans* asexual spores. *mBio* 12:e03128-20. <https://doi.org/10.1128/mBio.03128-20>.

**Editor** Xiaorong Lin, University of Georgia

**Copyright** © 2021 Wu et al. This is an open-access article distributed under the terms of the [Creative Commons Attribution 4.0 International license](https://creativecommons.org/licenses/by/4.0/).

Address correspondence to Hee-Soo Park, [phsoo97@knu.ac.kr](mailto:phsoo97@knu.ac.kr).

\* Present address: Ming-Yueh Wu, Ginkgo Bioworks Inc., Boston, Massachusetts, USA.

**Received** 5 November 2020

**Accepted** 21 December 2020

**Published** 9 February 2021

VelB TFs govern the coordination of morphological and chemical developments during sporogenesis. The results of this study provide insights into the interdependent, overlapping, or distinct genetic regulatory networks necessary to produce intact asexual spores. The findings are relevant for other *Aspergillus* species such as the major human pathogen *Aspergillus fumigatus* and the aflatoxin producer *Aspergillus flavus*.

**KEYWORDS** sporulation, asexual development, velvet, WetA, secondary metabolites, *Aspergillus*, transcription factor, genetic regulatory network

Fungal asexual spores are key reproductive cells that are essential for the long-term survival of filamentous fungi under a variety of environmental conditions (1). These spores can easily disperse into various environmental niches and act as infectious units for some pathogenic fungi (2–4). Asexual development in *Aspergillus* involves the formation of multicellular structures called conidiophores, each bearing hundreds of asexual spores called conidia. The production of intact conidia (conidiation) requires highly specialized cellular and structural differentiation and metabolic remodeling, which is governed by the coordinated activities of multiple positive and negative regulators (5, 6). Current knowledge about conidiogenesis is derived from numerous studies in model filamentous fungi such as *Aspergillus nidulans* (7–10).

The entire process of conidiogenesis is regulated by distinct gene sets, including central, upstream, and feedback regulators (6, 11). These components are highly conserved in *Aspergillus* species (12). In order to initiate conidiation, upstream developmental activators (FluG and FlbA, FlbB, FlbC, FlbD, and FlbE) induce the activation of *brlA*, an essential initiator of conidiation (13). This occurs when the fungal cells have acquired developmental competence that involves the removal of repressive effects imposed by the key negative regulators SfgA, NsdD, and VosA (14–16). Upon the activation of BrlA, it turns on AbaA and WetA, and together they sequentially control the conidiation-specific genetic regulatory networks, thereby governing the formation of conidiophores consisting of aerial stalks, vesicles, metulae, phialides, and conidia (9, 17). These three regulators are considered to form the central regulatory pathway (BrlA→AbaA→WetA) in *Aspergillus* species (18). BrlA is a key transcription factor (TF) that activates the expression of *abaA* and other genes in the early stage of conidiation (19, 20). AbaA is a TEF1 (transcriptional enhancer factor 1) family TF governing the expression of certain genes such as *wetA*, *vosA*, *velB*, and *rodA* in the metulae and phialides (21–23). WetA plays an important role in conidial wall integrity and conidial maturation during the late phase of conidiogenesis (24, 25). Our recent studies have shown that WetA functions as a DNA-binding protein that regulates spore-specific gene expression (25, 26). Along with WetA, two velvet regulators, VosA and VelB, which are fungus-specific TFs, coordinate morphological, structural, and chemical developments and exert feedback control of BrlA in conidia (27–30).

Previous studies have found that single-knockout mutants of *vosA*, *velB*, and *wetA* share multiple conidial phenotypes, including reduced spore viability, impaired trehalose biosynthesis, defective cell wall integrity, and reduced stress tolerance (25, 31, 32). The mRNA levels of these three regulators are high in wild-type (WT) conidia (25, 27, 28, 33). Results of chromatin immunoprecipitation (ChIP) analyses have demonstrated that VosA and WetA recognize certain DNA sequences in the promoter regions of target genes and regulate the mRNA expression of spore-specific genes in asexual spores (25, 29). In addition, the deletion of *vosA* or *wetA* affects the mRNA levels of multiple secondary metabolite cluster genes (25, 30, 34). Biochemical studies have determined that VosA interacts with VelB in conidia, and this complex controls trehalose and  $\beta$ -glucan biosynthesis (30, 35). Importantly, the roles of these three TFs are conserved in *Aspergillus* species (36–39). Considered jointly, these results suggest that VosA, VelB, and WetA are key TFs that orchestrate spore-specific gene expression in *A. nidulans*. Although the role of each regulator has been studied, the regulatory networks between these proteins have not, to date, been investigated in detail. In addition, the effects of these three proteins on primary and secondary metabolism are yet to be elucidated.

In this study, we aimed to determine the cross-regulatory mechanisms of VosA/VelB/WetA in fungal conidiation using comparative transcriptomic and metabolomic analyses of WT and null mutants of *wetA*, *velB*, and *vosA* in *A. nidulans* conidia. In addition, the direct targets of these regulators were identified by combining the results from the VosA- and VelB-chromatin interactions using ChIP sequencing (ChIP-seq) analysis with WetA direct targets identified in a previous study (25). The results clarify the detailed molecular mechanisms by which VosA/VelB and WetA control defined common and distinct regulons and increase the overall understanding of the regulatory networks that govern fungal cell differentiation and metabolism.

## RESULTS

**VosA-, VelB-, and WetA-mediated gene regulation in *A. nidulans* conidia.** To understand the conserved and divergent regulatory roles of VosA, VelB, and WetA in *A. nidulans* conidia, a comparative analysis of gene expression differences between the WT and null mutant conidia was carried out (Fig. 1). Totals of 40.98% (4,503/10,988), 45.61% (5,012/10,988), and 51.96% (5,729/10,988) of genes of the *A. nidulans* genome are differentially regulated in the  $\Delta vosA$ ,  $\Delta velB$ , and  $\Delta wetA$  mutant conidia, respectively, suggesting that the three regulators have a broad regulatory effect on conidia (see Fig. S1 in the supplemental material). A total of 2,143 differentially expressed genes (DEGs) between the WT and the  $\Delta vosA$ ,  $\Delta velB$ , and  $\Delta wetA$  mutant conidia were identified (Fig. 1A) (fold change of  $>2.0$  for upregulation or downregulation and  $q$  value [false discovery rate {FDR}] of  $<0.05$ ). The mRNA expression levels of 890 genes were downregulated in all three mutant conidia compared with the WT conidia. However, in all three mutant conidia, the mRNA levels of 1,253 genes were upregulated. Among them, the mRNA expression levels of a variety of genes associated with asexual development and signal transduction were affected by these three TFs (Tables S1 and S2). Certain developmental regulator genes such as *abaA*, *brlA*, *flbC*, *nosA*, *nsdC*, *velC*, *vapA*, and *esdC* were upregulated in all three null mutants (Table S1). Genes associated with heterotrimeric G-protein signal transduction (GprC, GprK, GprM, FlbA, and RgsB) and the mitogen-activated protein (MAP) kinase pathway (MpkB and ImeB) were also upregulated by these TFs in conidia (Table S2). However, several genes related to sporulation, spore wall formation, and structural integrity, including *rodA*, *conJ*, *tpsA*, *wA*, *vadA*, and *atfB*, were downregulated in all three null mutants (Table S1). Importantly, 748 and 769 DEGs were down- or upregulated by both  $\Delta vosA$  and  $\Delta velB$  mutant conidia, respectively, but not  $\Delta wetA$  mutant conidia, while the mRNA levels of 2,792 genes were affected solely in the *wetA*-null mutant conidia. Put together, these results suggest that VosA and VelB share more DEGs, while the WetA regulon has many more uniquely regulated genes.

To gain further insight into the regulatory roles of these TFs, functional category analyses using Gene Ontology (GO) terms were carried out (Fig. 1B). The results of the GO analysis demonstrated that several genes involved in the monocarboxylic acid metabolic process, the oxidation-reduction process, the trehalose metabolic process, and the cellular carbohydrate metabolic process were downregulated in all three mutant conidia, whereas a large number of genes associated with the secondary metabolic biosynthetic process, the chitin biosynthetic process, asexual sporulation resulting in formation, and the (1-3)- $\beta$ -D-glucan metabolic process were upregulated in these mutant conidia. The VosA- and VelB-specific downregulated genes were enriched in functional categories that included the cellular catabolic process, protein localization, and the acetate catabolic process. The functional GO categories associated with the VosA- and VelB-specific upregulated genes were the secondary metabolic biosynthetic process, the steroid metabolic process, and transport (Fig. S2A). Interestingly, a large number of genes involved in the RNA metabolic process were downregulated in  $\Delta wetA$  mutant conidia but not in  $\Delta vosA$  or  $\Delta velB$  mutant conidia (Fig. S2B).

**Putative direct targets of VosA, VelB, and/or WetA in conidia.** Our previous studies reported that VosA contains the velvet DNA-binding domain, which recognizes the VosA-binding motif in certain promoter regions (29). To identify the VelB direct target genes and compare the putative direct target genes of VosA and VelB, ChIP

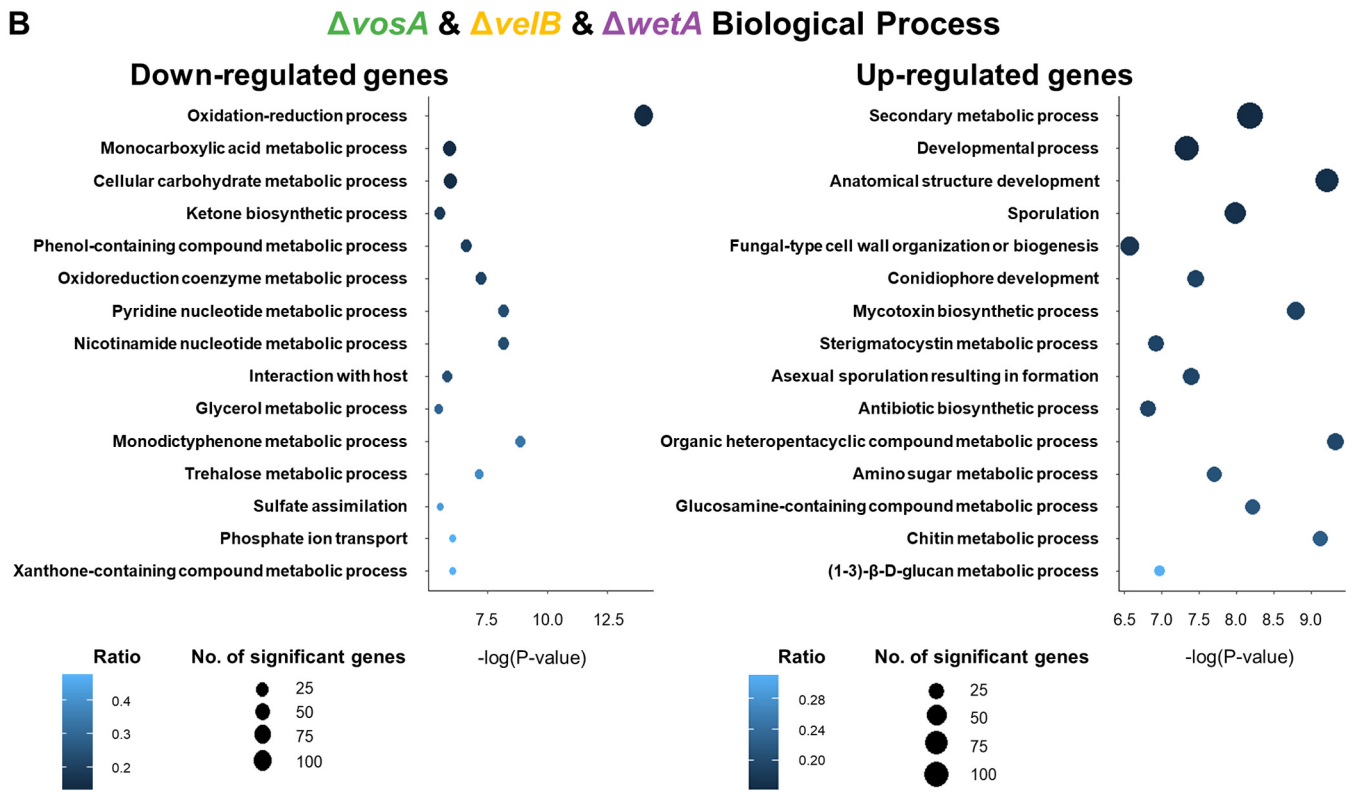
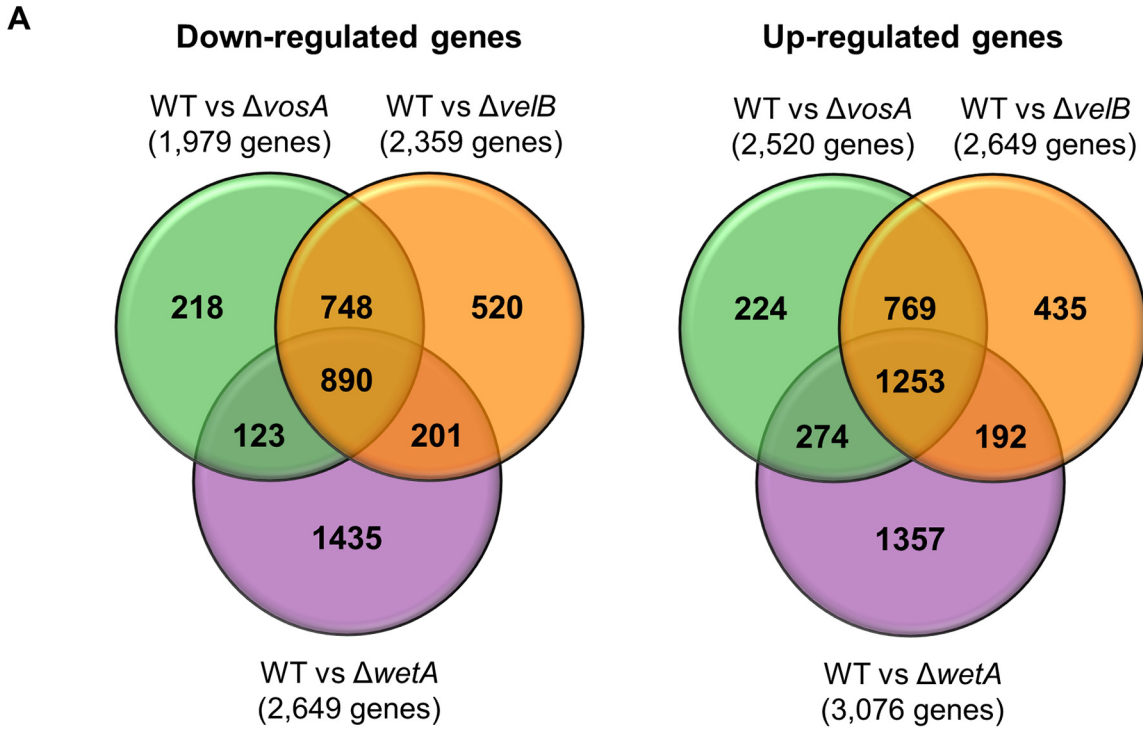
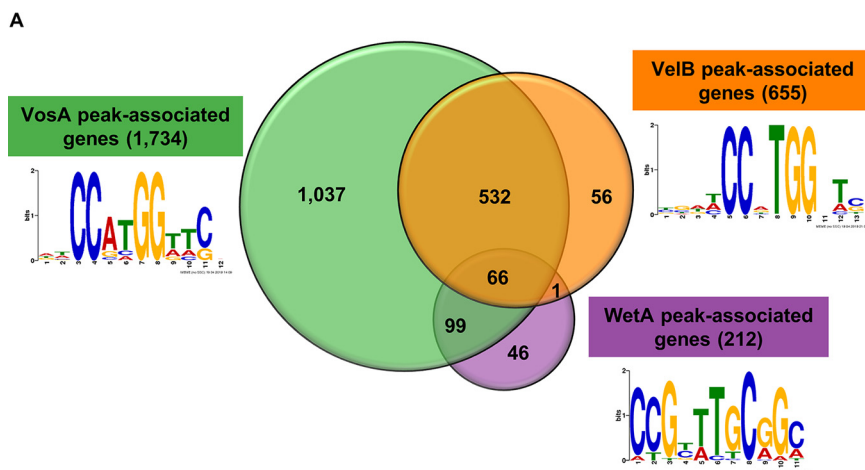


**FIG 1** Genome-wide analyses of the genes differentially affected by VosA, VelB, and WetA in *A. nidulans* conidia. (A) Venn diagram showing the genes whose mRNA levels are downregulated (left) or upregulated (right) by the absence of VosA, VelB, or WetA in conidia. (B) Gene Ontology (GO) term enrichment analysis of downregulated (left) or upregulated (right) genes in the  $\Delta vosA$ ,  $\Delta velB$ , and  $\Delta wetA$  conidia.

experiments followed by high-throughput sequencing of the enriched DNA fragments were carried out. ChIPs from strains containing FLAG epitope-tagged versions of VosA and VelB were compared to ChIPs from WT conidia that did not contain the FLAG epitope. Totals of 1,734 and 655 genes that were VosA and VelB peak associated,



**B**

Gene ID	logFC			Gene name	Gene description
	$\Delta wetA$	$\Delta vosA$	$\Delta velB$		
<b>Up-regulated genes</b>					
AN5893	4.08	2.96	2.02	<i>flbA</i>	RGS (regulator of G-protein signaling) family member
AN2385	1.15	5.03	3.76	<i>xgeA</i>	GPI anchored endo-1,3(4)-beta-glucanase
AN1058	5.20	4.26	3.87		SCP-like extracellular protein
AN2989	3.89	4.26	3.85		Glycine-rich RNA-binding protein
AN3674	6.71	4.19	4.14		PH domain protein
AN0378	3.82	1.29	1.33		Hypothetical protein
AN5756	2.90	3.48	3.14		Hypothetical protein
AN7101	2.70	2.04	1.83		Hypothetical protein
AN10458	5.25	2.03	2.09		Hypothetical protein
<b>Down-regulated genes</b>					
AN8643	-4.62	-3.99	-3.35	<i>atfB</i>	bZIP transcription factor
AN5523	-1.62	-1.65	-2.37	<i>tpsA</i>	Alpha,alpha-trehalose-phosphate synthase
AN5709	-6.86	-1.67	-3.72	<i>vadA</i>	Hypothetical protein
AN3079	-10.47	-2.23	-2.47	<i>cetA</i>	Extracellular thaumatin domain protein
AN3361	-1.16	-1.80	-2.46	<i>nopA</i>	G-protein coupled receptor-like protein
AN0129	-2.29	-1.01	-2.87	<i>ppsA</i>	Putative tyrosine phosphatase
AN2466	-2.36	-1.31	-2.04		MFS glucose transporter, putative
AN11917	-9.45	-1.89	-3.31		Has domain(s) with predicted O-methyltransferase activity
AN6403	-11.38	-2.62	-4.60		Hypothetical protein
AN7102	-6.96	-7.23	-6.48		Hypothetical protein
AN10040	-10.80	-9.74	-10.97		Hypothetical protein

**FIG 2** Identification of VosA, VelB, and WetA direct targets in *A. nidulans* conidia. (A) Venn diagram showing the number of the VosA, VelB, and WetA peak-associated genes in conidia. Motifs identified in peak-associated genes are shown next to the labels. (B) Summary of potential VosA, VelB, and WetA direct target DEGs in *A. nidulans* conidia. GPI, glycosylphosphatidylinositol; SCP, sperm-coating protein; PH, pleckstrin homology; bZIP, basic leucine zipper; MFS, major facilitator superfamily.

respectively, were identified using the same analysis pipeline as the one described previously (25) (Fig. 2). To identify the VosA/VelB response elements, DNA sequences in the 100 bp surrounding each peak were subjected to Multiple Em for Motif Elicitation (MEME) analysis, which led to the predicted VosA response element (VoRE) and the predicted VelB response element (VbRE) (Fig. 2A). Interestingly, the predicted VbRE (5'-CCXTGG-3') was quite similar to the predicted VoRE (5'-CCXXGG-3'). The VoRE was found in 278/1,404 peak sequences, had an E value of  $1.6e-56$ , and was the only motif identified by MEME with an E value of  $<1$ . The VbRE was found in 188/511 peak sequences, had an E value of  $2.4e-85$ , and was one of only two motifs identified by MEME with an E value of  $<1$  (the other motif had an E value of  $4.0e-5$  and was found in only 72 peak sequences).

We then compared the results of the ChIP-seq and RNA sequencing (RNA-seq) analyses to identify potential direct target genes of the three TFs (Table S3). There were 66 genes associated with the peaks of all three TFs (Table S4). Among them, 22 genes, including *flbA*, *xgeA*, *atfB*, *tpsA*, *vadA*, *cetA*, *nopA*, and *ppsA*, were DEGs in all three null mutants (Fig. 2B). Importantly, 532 genes were considered to be potential direct target



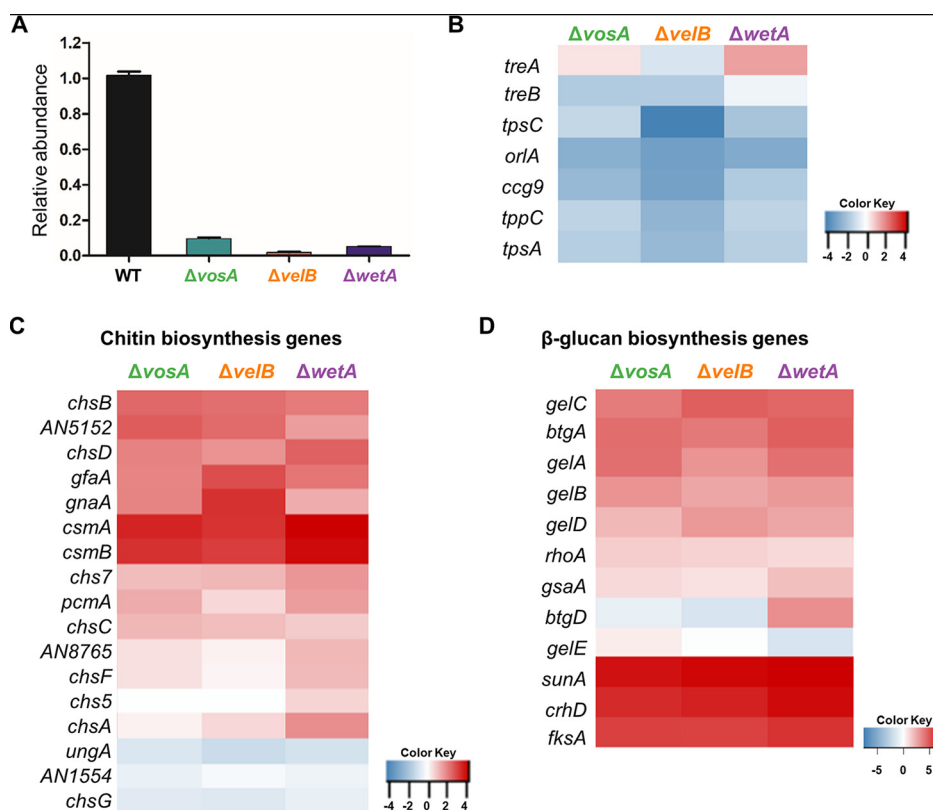


**FIG 3** Regulatory effects of VosA, VelB, and WetA on trehalose, chitin, and  $\beta$ -1,3-glucan biosynthesis in *A. nidulans* conidia. (A) Amount of conidial trehalose in *A. nidulans*. (B to D) Levels of mRNA of the genes associated with trehalose levels (B), chitin biosynthesis (C), and  $\beta$ -1,3-glucan biosynthesis (D) in the  $\Delta vosA$ ,  $\Delta velB$ , and  $\Delta wetA$  conidia. logFC, log fold change; GPI, glycosylphosphatidylinositol; MFS, major facilitator superfamily.

genes for both VosA and VelB but not WetA. A total of 166 genes were upregulated in both  $\Delta vosA$  and  $\Delta velB$  mutant conidia. These genes, including *brlA*, *fadaA*, *rosA*, *steA*, *steC*, and *veA*, were found to be involved primarily in asexual or sexual developmental processes. Taking these results together with the previously reported results (27, 35), we suggest that VosA works with VelB and that the VosA-VelB complex coordinates the processes involved in conidial production and maturation in *A. nidulans*.

**Roles of VosA, VelB, and/or WetA in conidial wall integrity.** Previous studies have shown that the deletion of *vosA*, *velB*, or *wetA* leads to decreased amounts of trehalose and increased  $\beta$ -glucan levels in conidia (25, 30). The results of transmission electron microscopy analyses revealed that three TFs are needed for the proper formation of the conidial wall (25, 30, 37), suggesting that these genes play a conserved role in regulating the expression of genes associated with conidial structural integrity. High-performance liquid chromatography (HPLC) analysis demonstrated that the trehalose contents of the three null mutant conidia were dramatically decreased (Fig. 3A). The mRNA expression levels of most genes involved in trehalose biosynthesis were downregulated (Fig. 3B and Table S5). In addition, *tpsA*, a putative trehalose synthase gene, is the direct target of three TFs (Fig. 2B). These results suggest that three TFs directly or indirectly control the mRNA levels of genes associated with trehalose biosynthesis, thereby regulating the trehalose contents in conidia. Most genes associated with chitin and  $\beta$ -(1,3)-glucan biosynthesis were upregulated in the  $\Delta vosA$ ,  $\Delta velB$ , and  $\Delta wetA$  mutant conidia (Fig. 3C and D). These results suggest that VosA, VelB, and WetA govern the mRNA expression of genes associated with conidial wall integrity in *A. nidulans*.

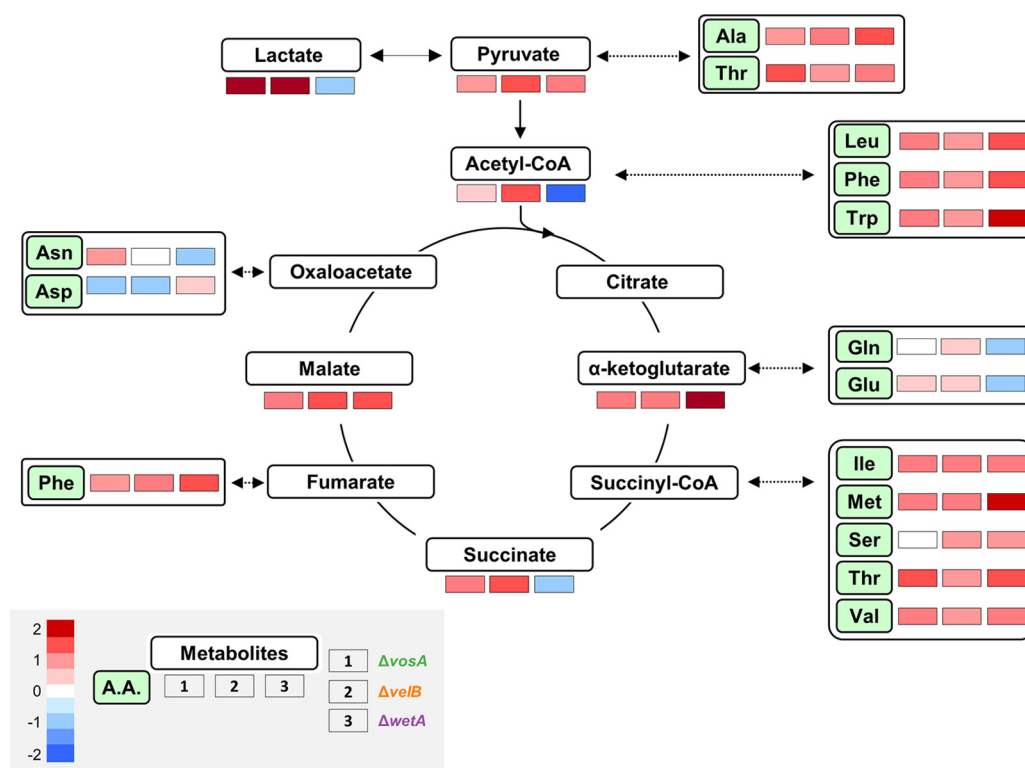


**FIG 4** Roles of VosA, VelB, and WetA in primary metabolism of *A. nidulans* conidia. Shown are maps of primary metabolites involved in the TCA cycle and amino acid (A.A.) biosynthesis in WT,  $\Delta vosA$ ,  $\Delta velB$ , and  $\Delta wetA$  conidia. Levels of identified primary metabolites produced in the WT and null mutant conidia are shown.

**Alterations to primary metabolites in  $\Delta vosA$ ,  $\Delta velB$ , and  $\Delta wetA$  conidia.** As mentioned above, the deletion of *vosA*, *velB*, or *wetA* led to alterations in the mRNA expression of genes involved in metabolic processes (glycerol metabolic process, ketone metabolic process, and amino sugar metabolic process) and amino acid metabolism (Table S6), implying that the amounts of primary metabolites may be affected by the absence of *vosA*, *velB*, or *wetA* in conidia. To test this hypothesis, the abundances of several primary metabolites involved in the tricarboxylic acid (TCA) cycle and amino acid biosynthesis were examined in WT and mutant conidia (Fig. 4). The abundances of pyruvate,  $\alpha$ -ketoglutarate, and malate were increased in the conidia of the three null mutants. The abundances of acetyl-CoA and succinate were decreased in both  $\Delta vosA$  and  $\Delta velB$ , but not  $\Delta wetA$ , mutant conidia. The amounts of lactate in both  $\Delta vosA$  and  $\Delta velB$  mutant conidia were significantly large compared with those in WT conidia.

The abundances of 13 amino acids (alanine, isoleucine, methionine, leucine, phenylalanine, tryptophan, valine, threonine, serine, asparagine, glutamine, aspartate, and glutamate) were affected in at least one null mutant. Moreover, the levels of nine amino acids were high in all three mutant conidia. The effects of deleting *vosA-velB* or *wetA* on the abundances of glutamate, glutamine, aspartate, and asparagine differed. The deletion of *wetA* caused decreased levels of glutamate, glutamine, and asparagine in conidia, whereas the levels of these amino acids were increased or not affected by the absence of *vosA* or *velB*. The genes involved in the biosynthesis of these amino acids and primary metabolites were differentially regulated in the three null mutants. Overall, these results show that WetA, VosA, and VelB regulate the expression of genes involved in both the TCA cycle and amino acid biosynthesis; however, the three lists of primary metabolites that they affect contain both shared and unique molecules.

**Abundances of secondary metabolites in  $\Delta vosA$ ,  $\Delta velB$ , and  $\Delta wetA$  conidia.** Previous studies found that these three TFs are important for the production of several

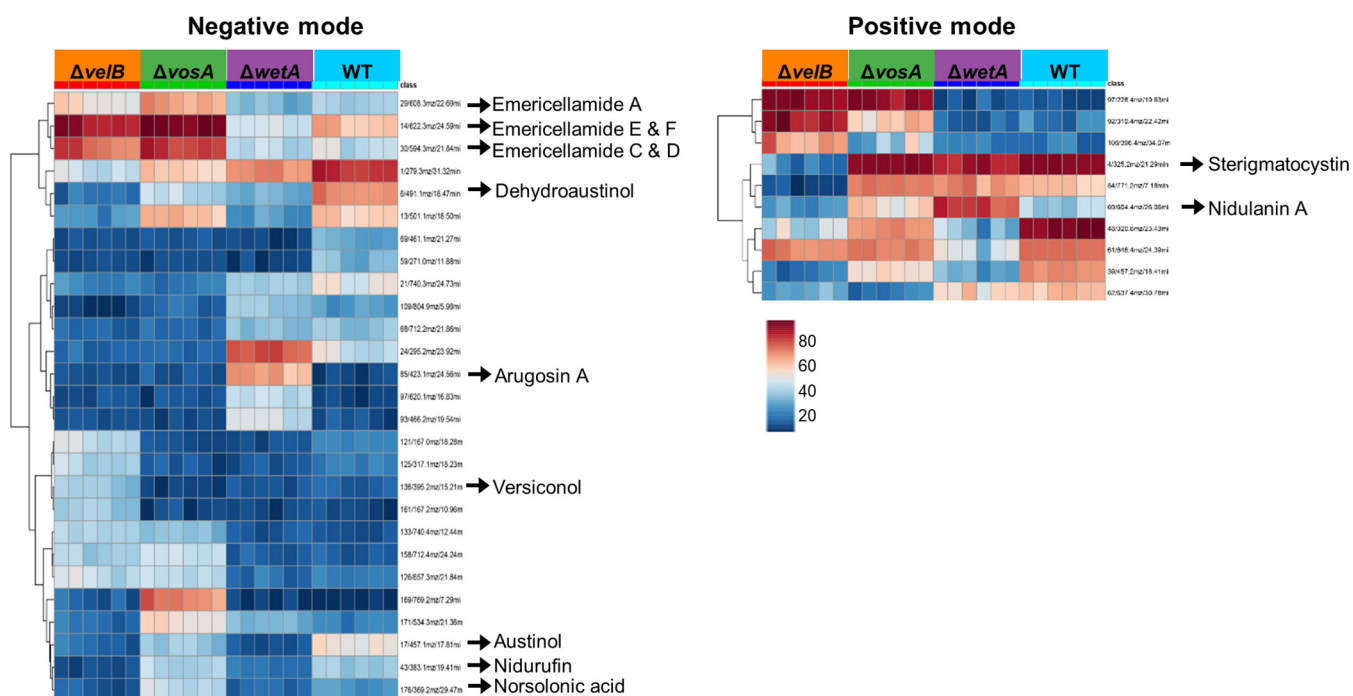


**FIG 5** Levels of secondary metabolites in the  $\Delta vosA$ ,  $\Delta velB$ , and  $\Delta wetA$  conidia. Differentially regulated secondary metabolites in WT,  $\Delta vosA$ ,  $\Delta velB$ , and  $\Delta wetA$  conidia are shown. The heat map is color-coded and represents high abundances (red) or low abundances (blue) of ions/retention time pairs detected by LC-MS analysis.

secondary metabolites in *Aspergillus* species (34, 36, 40). In addition, according to the GO analysis results, the deletion of *vosA*, *velB*, or *wetA* results in an alteration of the mRNA expression of biosynthetic gene clusters involved in the production of multiple secondary metabolites, including monodictyphenone, sterigmatocystin, and asperfuranone (Fig. 1, Fig. S2, and Table S7). To elucidate the conserved and divergent regulatory effects of secondary metabolism in the three conidial mutants, the secondary metabolites were extracted and subjected to liquid chromatography-mass spectrometry (LC-MS) analysis. A principal-component analysis showed differences between the four different conidial samples (Fig. S3). The secondary metabolite content of the WT conidia was relatively similar to that of the  $\Delta wetA$  conidia, indicating similar abundances and types of secondary metabolites. Conidia from the  $\Delta vosA$  and  $\Delta velB$  mutants clustered far apart, which suggested that a unique set of secondary metabolites or different levels of metabolites were expressed and extracted. This is interesting considering that the two TFs can interact and that their binding motifs and regulated gene lists were so similar to one another (Fig. 1A and Fig. 2A).

Next, we applied analysis of variance to identify the most different molecular entities detected as mass/charge ( $m/z$ ) values and retention time (RT) pairs in the LC-MS analysis-derived metabolomics data. As shown in Fig. 5, the abundances of several secondary metabolites were different in the positive and negative ionization modes. For example, the abundance of arugosin A was high in the  $\Delta wetA$  conidia, compared with the WT conidia, but not in the  $\Delta vosA$  and  $\Delta velB$  mutant conidia.

To further dissect the roles of *VosA*, *VelB*, and *WetA* in secondary metabolism, we focused on some known secondary metabolites, including sterigmatocystin, emericellamide, and austinol (Fig. 6). Sterigmatocystin is a precursor of aflatoxins, and its biosynthetic gene cluster and intermediates have previously been studied (41, 42). The amount of sterigmatocystin in the  $\Delta velB$  conidia was significantly decreased compared with that in the WT conidia, but the  $\Delta vosA$  and  $\Delta wetA$  conidia contained similar amounts of sterigmatocystin (Fig. 6A). However, the amounts of sterigmatocystin intermediates were different in  $\Delta vosA$  and  $\Delta wetA$  conidia. Levels of norsolorinic acid and nidurufin were low in the  $\Delta velB$  and  $\Delta wetA$  conidia, while the level of versiconol was



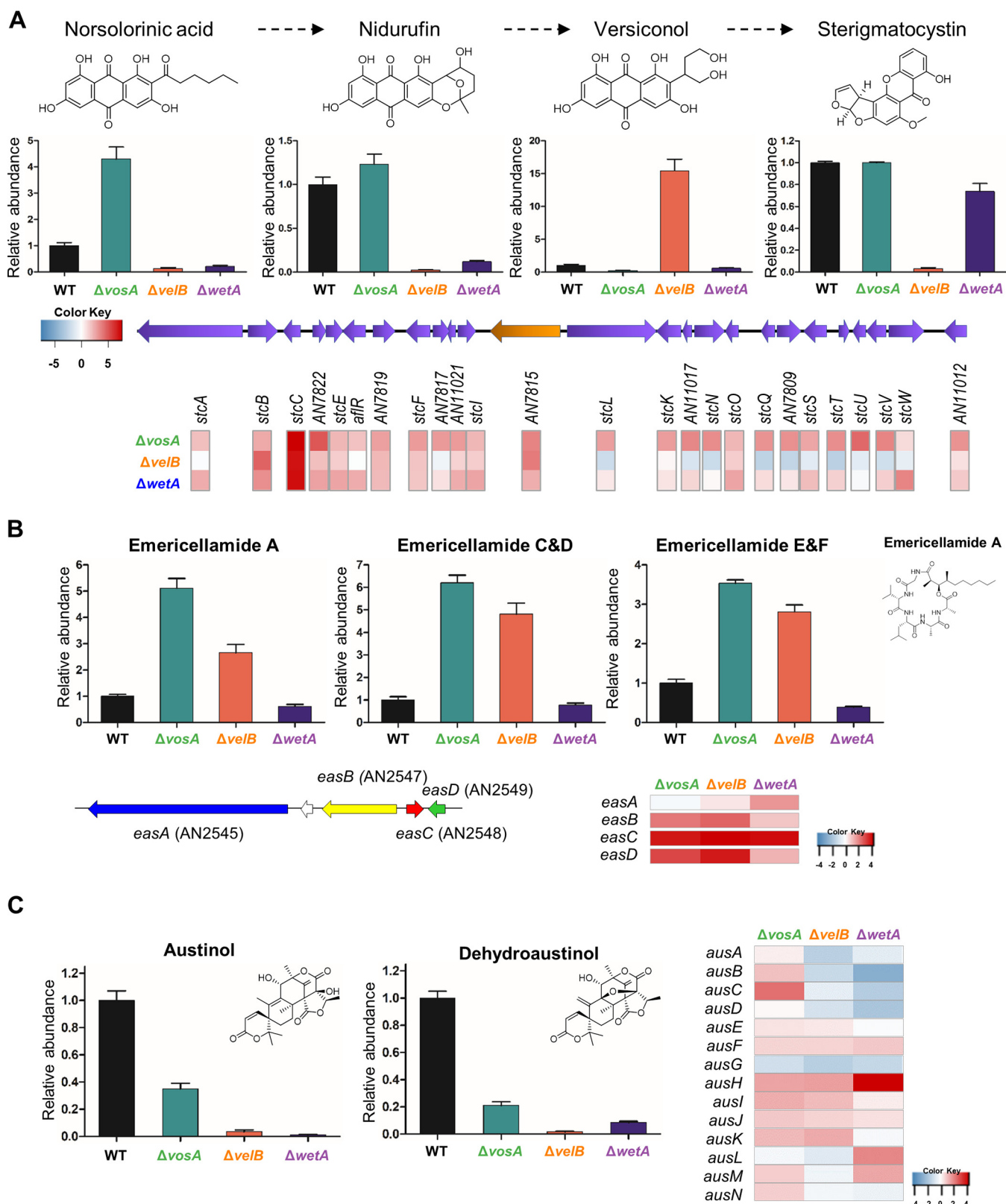


**FIG 6** Regulation of key secondary metabolites in  $\Delta vosA$ ,  $\Delta velB$ , and  $\Delta wetA$  conidia of *A. nidulans*. (A, top) Chemical structures of the compounds. (Middle) Abundances of norsolorinic acid, nidurufin, versiconol, and sterigmatocystin in WT,  $\Delta vosA$ ,  $\Delta velB$ , and  $\Delta wetA$  conidia. (Bottom) The sterigmatocystin gene cluster and differentially expressed genes involved in sterigmatocystin biosynthesis in  $\Delta vosA$ ,  $\Delta velB$ , and  $\Delta wetA$  conidia. (B, top) Abundance of emericellamide in WT,  $\Delta vosA$ ,  $\Delta velB$ , and  $\Delta wetA$  conidia with the emericellamide A structure. (Bottom) The emericellamide gene cluster and mRNA expression of genes associated with emericellamide biosynthesis in  $\Delta vosA$ ,  $\Delta velB$ , and  $\Delta wetA$  conidia. (C, left) Abundances of austinol and dehydroaustinol in WT,  $\Delta vosA$ ,  $\Delta velB$ , and  $\Delta wetA$  conidia with their structures. (Right) The austinol gene cluster and mRNA expression of genes associated with austinol biosynthesis in  $\Delta vosA$ ,  $\Delta velB$ , and  $\Delta wetA$  conidia.

high only in the  $\Delta velB$  conidia. The RNA-seq results indicated that the mRNA levels of almost all of the genes in the sterigmatocystin gene cluster were increased in both the  $\Delta vosA$  and  $\Delta wetA$  conidia, whereas the mRNA expression of these genes in the  $\Delta velB$  conidia was less consistent. In particular, the mRNA levels of *stcL*, *stcN*, *stcQ*, *stcS*, *stcT*, *stcU*, *stcV*, and *stcW* were decreased in the  $\Delta velB$  conidia compared with the WT conidia. These results suggest that VosA and VelB play diverse roles in the regulation of sterigmatocystin biosynthesis.

Emericellamide compounds are cyclopeptides that are produced by several *Aspergillus* species (43, 44). The abundances of these compounds, relative to WT production, were high in  $\Delta vosA$  and  $\Delta velB$  conidia, and the mRNA levels of *easA*, *easB*, *easC*, and *easD* were also high in both mutant conidia, implying that VosA and VelB repress emericellamide biosynthesis in WT conidia (Fig. 6B). In the  $\Delta wetA$  conidia, however, the mRNA expression of the emericellamide gene cluster was increased, but the quantity of emericellamide compounds did not increase, suggesting that the regulatory mechanism of emericellamide biosynthesis in the  $\Delta wetA$  conidia is more complex than the influence of  $\Delta vosA$  and  $\Delta velB$  on emericellamide production in conidia. In the three types of null mutant conidia, the abundances of two fungal meroterpenoids, austinol and dehydroaustinol (45), were decreased, compared with the WT conidia (Fig. 6C). Furthermore, the expression levels of several austinol cluster genes were decreased in the  $\Delta velB$  and  $\Delta wetA$  conidia. Taken together, these results demonstrate that the ways in which VosA, VelB, and WetA govern the expression of secondary metabolite gene clusters, and the production of their associated metabolites, in *A. nidulans* conidia are divergent from one another.

## DISCUSSION

Asexual developmental processes in filamentous fungi are regulated by a variety of TFs (6). These TFs orchestrate the spatial and temporal transcriptional expression of development-specific genes, leading to physiological and metabolic changes. During the processes of conidium formation from phialides and conidial maturation, conidium-specific TFs, including VosA, VelB, and WetA, regulate spore-specific gene expression patterns and metabolic changes (25, 30). In this study, we investigated the transcript and metabolite changes that are regulated by VosA, VelB, and WetA in *A. nidulans* conidia.

Transcriptomic analyses indicated that about 20% of the *A. nidulans* genome (2,143 genes) is differentially expressed in  $\Delta vosA$ ,  $\Delta velB$ , and  $\Delta wetA$  mutant conidia. ChIP-seq results identified 66 direct target genes that are shared between VosA, VelB, and WetA in conidia. These results offered some explanation of how these TFs control phenotypic changes in conidia. First, the deletion of *vosA*, *velB*, or *wetA* caused increased mRNA expression of certain development-specific genes, including *abaA* (23), *brlA* (19), *flbA* (46), *flbC* (47), *nsdC* (48), *nosA* (49), and *mpkB* (50), which are involved in the formation of asexual and sexual structures during the early and middle stages of conidium formation, but decreased transcript accumulation of spore-specific genes such as *vadA* (51), *catA* (52), *wA* (53), *conF* (54), *conJ* (54), *cetA* (55), *cetJ* (56), and *cetL* (56), which are important for conidial germination, morphogenesis, and dormancy (see Table S1 in the supplemental material). Alteration of the mRNA expression levels of development-specific genes or spore-specific genes affect spore maturation, dormancy, and germination. For example, misscheduled expression of key asexual developmental regulators, especially BrlA and AbaA, can affect proper sporulation (9, 57). In the case of the spore-specific genes, the deletion of *vadA* or *catA* affects conidial germination and the conidial stress response (51, 52, 58). Based on these results, we propose that alteration of the mRNA expression levels of development-specific genes or spore-specific genes caused by the deletion of *vosA*, *velB*, or *wetA* affect conidial maturation, dormancy, morphology, and germination. However, the detailed molecular mechanism of how three TFs act as activators or repressors for the expression of development-specific genes and spore-specific genes will be elucidated in further studies.

Another important phenotype of the  $\Delta vosA$ ,  $\Delta velB$ , and  $\Delta wetA$  mutant conidia was the differences in conidial wall integrity and the components of the conidial wall (25, 30). As shown in Fig. 3, most of the genes involved in chitin and  $\beta$ -glucan biosynthesis were upregulated in all three mutant conidia. The dynamic expression of these genes is required mainly for the remodeling of the cell wall during isotropic growth and mobilization of energy for differentiation (59) but is not required in dormant conidia. However, by altering the mRNA expression of these genes in the mutant conidia, the dormancy of conidia could be broken, affecting long-term viability as well as conidial germination.

Another feature of fungal spores is their ability to resist various environmental stresses (1). However,  $\Delta vosA$ ,  $\Delta velB$ , and  $\Delta wetA$  mutant conidia are more sensitive to several environmental stresses (25, 35). It is speculated that this is regulated by alterations in the expression of genes involved in environmental stress tolerance. The data that we show here support this hypothesis. First, these regulators govern the mRNA expression of genes involved in the trehalose biosynthetic pathway, thereby affecting the amount of conidial trehalose, a key component in stress protection and fungal virulence (60). Second, VosA, VelB, and WetA directly or indirectly regulate genes previously associated with stress responses. CatA is a spore-specific catalase, and compared with WT spores, *catA* deletion mutant spores are sensitive to oxidative stress (52). AtfB is a bZIP TF (61), and the AtfB homolog is crucial for the stress response in *Aspergillus oryzae* conidia (62). These two genes are putative direct target genes of the three regulators reported in this study, and the mRNAs of *catA* and *atfB* can be positively regulated by VosA, VelB, and WetA in conidia (Fig. 2 and Table S3). Along with these genes, the mRNA level of *hogA*, a key component of osmotic stress signaling (63), was downregulated in all mutant conidia. These results contribute to our understanding of the ways in which these three regulators influence the environmental stress response in conidia.

VosA, VelB, and WetA are key functional regulators in the formation of conidia and control spore-specific gene expression. However, our data have shown that their gene regulation networks are slightly different. RNA-seq results showed that VosA and VelB coregulate the expression of spore-specific genes. Importantly, the predicted VbRE is quite similar to the predicted VoRE (Fig. 2A). In addition, biochemical results from previous studies (27, 35) suggested that VosA and VelB form a heterocomplex in asexual spores. However, WetA is not directly related to VosA and VelB. WetA's putative binding site is different from the VosA/VelB binding site. Moreover, the WetA peak-associated genes and the VosA/VelB peak-associated genes did not overlap much. These results imply that WetA-mediated gene regulation may be different from the VosA- or VelB-mediated gene regulatory network.

The velvet domain is a fungus-specific DNA-binding domain that recognizes specific DNA sequences. Previously, Ahmed et al. proposed that the VosA velvet domain recognizes a DNA sequence (5'-TGGCCGCGG-3') based on ChIP-chip analysis and electrophoretic mobility shift assays (EMSAs) (29). Further EMSAs demonstrated that both TGG and CCGCGG sequences are necessary for DNA binding of the VosA velvet domain. In the present study, we conducted ChIP-seq analyses in conidia and proposed the predicted VbRE (5'-CCXTGG-3') and VoRE (5'-CCXXGG-3') (Fig. 2). In our experimental results, the TGG sequence does not appear for the VbRE or VoRE, but the 5'-CCXXGG-3' sequence is conserved in the VbRE and VoRE. The reason why these DNA sequences are not the same is likely because the experimental methods and analyses are different from those used to obtain the previous results. Ahmed et al. used 15 DNA sequences based on chromatin immunoprecipitation with microarray technology (ChIP-chip) analysis and EMSAs, whereas the motif in Fig. 2A was built from running MEME with every peak sequence that we identified. Nevertheless, the 5'-CCXXGG-3' sequence appears common in previous and current results. Based on these data, we propose that the 5'-CCXXGG-3' sequence may be crucial for DNA binding of the velvet

domain, and further studies will be needed to fine-tune the precise velvet protein-binding sequence.

During the asexual development of *A. nidulans*, the abundance of amino acids other than phenylalanine changes, and the expression of genes related to amino acid biosynthesis is altered (64). Overall, our analyses confirmed that the amounts of most amino acids, and the expression of related genes, increased in all mutant spores. In addition, the abundances of metabolites involved in the TCA cycle increased in all mutant conidia. However, the abundances of some primary metabolites such as glutamate, glutamic acid, lactate, and acetyl-CoA were decreased in the  $\Delta wetA$  conidia (Fig. 4). It is not yet clear how these metabolic changes affect spore production and maturation, and further studies will be needed to understand this.

Our multi-omics analyses found that VosA, VelB, and WetA regulate the expression of several secondary metabolite gene clusters (Table S7) and the production of secondary metabolites, especially sterigmatocystin, in conidia. The process of sterigmatocystin production and its regulation involves 25 genes, and this metabolite is produced via steps involving several intermediate products. In  $\Delta vosA$  conidia, the mRNA expression of sterigmatocystin gene clusters was induced, and the amounts of sterigmatocystin produced were similar to those in the WT conidia. These results were similarly observed in sexual spores (34). While the  $\Delta vosA$  conidia contained sterigmatocystin, the metabolite was not detected in  $\Delta velB$  conidia. We reported that the VosA-VelB complex is a functional unit in conidia, but this particular result indicates that VosA and VelB play different roles in sterigmatocystin production. It is possible that VelB forms another complex, such as the VelB-VeA-LaeA complex (40), to participate in sterigmatocystin production in conidia. For the  $\Delta velB$  conidia, we speculated that the mRNA expression levels of genes such as *stcB*, *stcC*, *stcF*, and *stcI*, which are associated with the early stages of sterigmatocystin biosynthesis, were increased, and that the amount of versiconol, a putative sterigmatocystin/aflatoxin intermediate, was also increased in comparison with the WT. However, the mRNA levels of genes associated with the late phase of sterigmatocystin biosynthesis, such as *stcL*, *stcN*, *stcQ*, and *stcT*, were decreased in  $\Delta velB$  conidia. It might be possible that VelB (or VelB/VeA/LaeA) can regulate some expression of sterigmatocystin gene clusters by epigenetic means rather than through the canonical method of *affR* expression or activity. Although changes in the expression of secondary metabolite gene clusters and secondary metabolites affected by three TFs were studied, detailed molecular mechanisms have not been studied yet. Therefore, it is necessary to study how these three TFs work together or separately through further research. In the  $\Delta vosA$  and  $\Delta wetA$  conidia, the mRNA levels of most of the genes in the sterigmatocystin gene cluster were increased compared to those in WT conidia, but the amounts of sterigmatocystin were similar to those in WT conidia. There are some speculations about this phenomenon. The expression of genes may not directly affect the biosynthesis of secondary metabolites. Alternatively, the translation of mRNA molecules to proteins and the posttranslational modification of those metabolite-producing proteins are two factors that can create discrepancies between RNA and metabolite abundances. To further explain this, further experiments should be conducted to determine how the three TFs regulate the biosynthesis of secondary metabolites.

In conclusion, this study provides a systematic dissection of the gene regulatory network and molecular mechanisms of VosA, VelB, and WetA (Fig. 7). In conidia, VosA, VelB, and WetA directly or indirectly control the expression of spore-specific or development-specific genes, thereby altering conidial wall integrity and conidial viability. In addition, these TFs regulate multiple secondary metabolite gene clusters, thus inducing secondary metabolic changes. These results provide an advance in the knowledge of conidial formation and will provide the basis for future insights into spore formation in other filamentous fungi.

## MATERIALS AND METHODS

**Strains, media, and culture conditions.** The fungal strains used in this study are listed in Table 1. Fungal strains were grown on solid or liquid minimal medium with 1% glucose (MMG) and appropriate

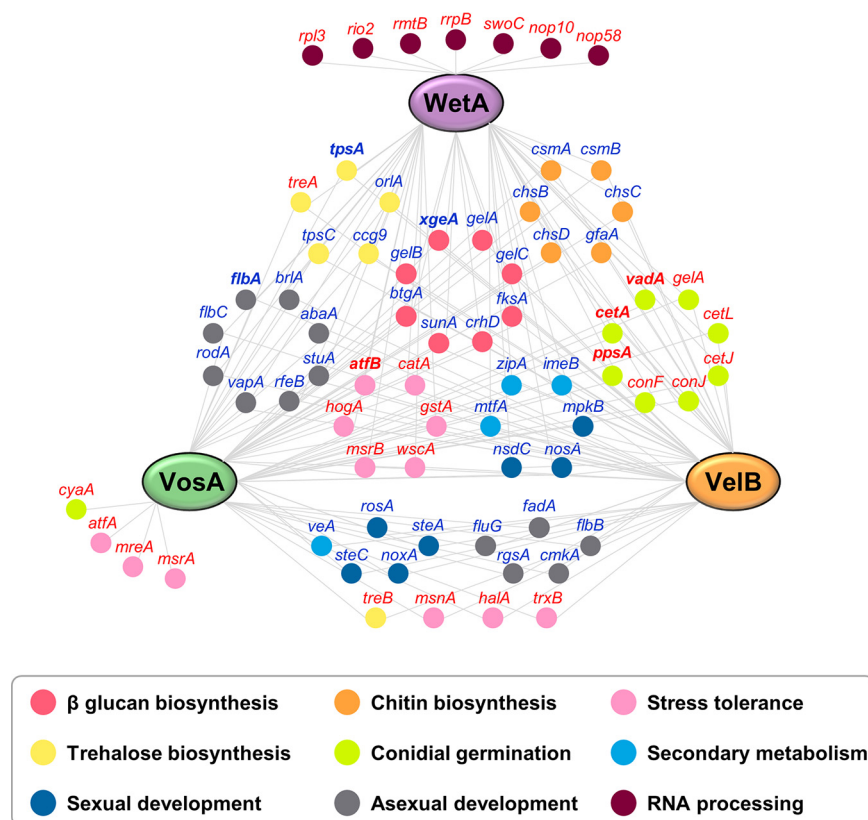


**FIG 7** Proposed gene regulatory network of VosA, VelB, and WetA in conidia. The network represents the interactions between VosA/VelB/WetA and their target genes. Gene names in boldface type are direct target genes of all three TFs. Gene names in red or blue are genes induced or repressed, respectively, by VosA, VelB, and/or WetA in conidia.

supplements for general purposes as previously described (65). For conidium samples, WT and mutant conidia were inoculated onto solid MMG plates and incubated for 48 h. Next, conidia were collected from plates using Mira cloth (Calbiochem, San Diego, CA, USA) and stored at  $-80^{\circ}\text{C}$ .

**RNA sequencing analysis.** To isolate total RNA for RNA sequencing (RNA-seq) analysis, total RNA from WT and mutant conidia was extracted using TRIzol reagent (Invitrogen, USA), according to the manufacturer's instructions, with modifications. To remove DNA contamination from the RNA samples, DNase I (Promega, USA) was added, and RNA was then purified using an RNeasy minikit (Qiagen, USA). Three technical replicates of each sample were analyzed. RNA sequencing was performed as previously described (34). RNA samples were submitted to the University of Wisconsin Gene Expression Center (Madison, WI, USA) for library preparation and sequencing. A strand-specific library was prepared using an Illumina TruSeq strand-specific RNA sample preparation system. The libraries of all the replicates were sequenced using an Illumina HiSeq 2500 system.

Data analysis of the  $\Delta\text{vosA}$  and  $\Delta\text{velB}$  RNA-seq experiments was performed using the same analysis pipeline as the one previously described for the  $\Delta\text{wetA}$  RNA-seq analysis (25). Reads were mapped to the *A. nidulans* FGSC4 transcriptome using Tophat2 version 2.1.1 (66) and the parameter “-max-intron-length 4000.” On average, 19.9 million reads per sample mapped to the genome, and the number of reads aligning to each gene was counted with HTseq-Count version 0.9.1 (67). DESeq version 1.14.1 (68)

**TABLE 1** *Aspergillus* strains used in this study

Strain	Relevant genotype	Source or reference
FGSC4	<i>A. nidulans</i> wild type; <i>veA</i> <sup>+</sup>	FGSC <sup>a</sup>
THS15	<i>pyrG89</i> ; <i>pyroA4</i> ; $\Delta\text{vosA}::\text{AfupyrG}^+$ ; <i>veA</i> <sup>+</sup>	27
THS16	<i>pyrG89</i> ; <i>pyroA4</i> ; $\Delta\text{velB}::\text{AfupyrG}^+$ ; <i>veA</i> <sup>+</sup>	27
THS20.1	<i>pyrG89</i> ; <i>pyroA</i> :: <i>velB(p)::velB::FLAG</i> <sub>3x</sub> :: <i>pyroA</i> <sup>b</sup> ; $\Delta\text{velB}::\text{AfupyrG}^+$ ; <i>veA</i> <sup>+</sup>	27
THS28.1	<i>pyrG89</i> ; <i>pyroA</i> :: <i>vosA(p)::vosA::FLAG</i> <sub>3x</sub> :: <i>pyroA</i> <sup>b</sup> ; $\Delta\text{vosA}::\text{AfupyrG}^+$ ; <i>veA</i> <sup>+</sup>	27
TMY4	<i>pyrG89</i> ; <i>pyroA4</i> ; $\Delta\text{wetA}::\text{AfupyrG}^+$ ; <i>veA</i> <sup>+</sup>	25

<sup>a</sup>FGSC, Fungal Genetic Stock Center.

<sup>b</sup>The 3/4 *pyroA* marker causes targeted integration at the *pyroA* locus.



was used to determine significantly differentially expressed genes, and genes were considered regulated if they exhibited an adjusted  $P$  value of  $<0.05$  and a  $\log_2$  fold change either greater than 1 or less than  $-1$ .

**Chromatin immunoprecipitation sequencing analysis.** Samples for chromatin immunoprecipitation sequencing (ChIP-seq) analysis were prepared according to methods described previously (29, 30). DNA samples from each strain were extracted using a MAGnify chromatin immunoprecipitation system (Invitrogen, USA) according to the manufacturer's protocol, with modification. Two-day-old conidia from the WT strain or strains containing VosA-FLAG or VelB-FLAG were cross-linked, washed, homogenized with a Mini-Beadbeater 16 instrument (Biospec, USA), sonicated, and separated by centrifugation. The chromatin extracts were incubated with an anti-FLAG antibody–Dynabead complex. Next, samples were eluted from the beads at 55°C using proteinase K. Enriched DNA was purified using DNA purification magnetic beads. DNA samples from each strain were submitted to the University of Wisconsin Gene Expression Center (Madison, WI). Libraries were prepared using a TruSeq ChIP library preparation kit (Illumina, CA). The libraries of all the replicates were sequenced using an Illumina HiSeq 2500 system.

Raw reads were trimmed using Trimmomatic version 0.36 (69) and the parameters "ILLUMINACLIP:2:30:10 LEADING:3 TRAILING:3 SLIDINGWINDOW:4:15 MINLEN:36." Trimmed reads were mapped to the *A. nidulans* A4 genome using version 0.7.15 of BWA-MEM (70), and shorter split hits were marked as secondary alignments. Mapped reads with mapping quality (MAPQ) values of  $<1$  as well as unmapped, secondarily aligned, supplementary, and duplicated reads were discarded with SAMtools version 1.6 (71). On average, 2.3 million and 7.2 million reads per sample were used for peak calling in the VosA and VelB experiments, respectively. Mapped reads that survived our filter were pooled, and extension sizes were estimated with version 1.15.2 of SPP (72, 73). Peaks were called with MACS2 (74) version 2.1.2 using the extension sizes estimated by SPP, a genome size of 2.93e7, and the "–nomodel" parameter. Peaks with a fold change of  $>2.0$  and a  $q$  value of  $<0.001$  were further analyzed. Peak lists were combined from both of the VosA biological replicates, as  $>99\%$  of the peaks from the first replicate were found in the second replicate. Motifs were identified in the 100 bp of sequences surrounding each peak summit using MEME-ChIP (75). Motifs that occurred zero times or once in the sequences around the peaks and that were 4 to 21 nucleotides (nt) long were further analyzed.

**Functional enrichment analysis.** Enriched terms from the GO Biological Process, KEGG, InterPro, and Pfam databases were identified using the tools available at AspGD (76), FungiDB (77), and ShinyGO v0.60 (78). Unless otherwise stated, default settings were used in ShinyGO v0.60. The settings were as follows: database, *Emmericella nidulans* STRINGdb;  $P$  value cutoff (FDR), 0.05; number of most significant terms to show, 30.

**Primary metabolite analysis.** WT and  $\Delta wetA$ ,  $\Delta vosA$ , and  $\Delta velB$  mutant conidia were inoculated onto solid MMG plates and incubated for 48 h, and fresh conidia were then harvested using MiraCloth with HPLC-grade water. For each sample,  $2 \times 10^8$  conidia were mixed with 500  $\mu$ l HPLC-grade acetonitrile-methanol-water (40:40:20, vol/vol) and 300  $\mu$ l beads, homogenized by using the Mini-Beadbeater, and centrifuged. The supernatant was filtered using a 0.45- $\mu$ m polytetrafluoroethylene (PTFE) Mini-UniPrep filter vial (Agilent), collected, and immediately snap-frozen with liquid nitrogen. The samples were stored at  $-80^\circ\text{C}$  until primary metabolite analysis.

The samples were then analyzed as described previously (79, 80). Samples were analyzed using an HPLC-MS system consisting of a Dionex ultrahigh-performance liquid chromatography (UHPLC) instrument coupled by electrospray ionization (ESI) (negative mode) to a hybrid quadrupole–high-resolution mass spectrometer (Q Exactive orbitrap; Thermo Scientific) operated in full-scan mode. Metabolite peaks were identified by their exact mass and matching retention times to those of pure standards (Sigma-Aldrich).

**Secondary metabolite analysis.** The conidia of WT and  $\Delta wetA$ ,  $\Delta vosA$ , and  $\Delta velB$  mutant strains were extracted by adding 1.5 ml of a methanol-acetonitrile (2:1) mixture followed by sonication for 60 min. The suspension was then left overnight before centrifugation at 14,000 rpm for 15 min. The supernatant (1 ml) was removed, filtered, and evaporated to dryness *in vacuo*. Extracts for the metabolomics analysis were normalized to 10 mg/ml in methanol for LC-MS analysis.

Analytical HPLC was performed using an Agilent 1100 HPLC system equipped with a photodiode array detector. The mobile phase consisted of ultrapure water (mobile phase A) and acetonitrile (mobile phase B) with 0.05% formic acid in each solvent. A gradient method from 10% mobile phase B to 100% mobile phase B in 35 min at a flow rate of 0.8 ml/min was used. The column (Phenomenex Kinetex C<sub>18</sub>, 5  $\mu$ m by 150 mm by 4.6 mm) was reequilibrated before each injection, and the column compartment was maintained at 30°C throughout each run. All samples were filtered through a 0.45- $\mu$ m nylon filter before LC-MS analysis.

Extracts from the WT and mutant conidia were analyzed in duplicate on an Agilent 1100 series LC-MS platform (81, 82). The negative ionization mode was found to detect the most metabolites. The first 5 min of every run was removed due to a large amount of coeluting, low-molecular-weight, polar metabolites. Data sets were exported from Agilent's Chemstation software as .netCDF files and imported into MZmine 2.38 (83). Peak picking was performed with established protocols (84), resulting in 123 marker ions. Briefly, mass detection was centroid with a 5e2 minimum height. Chromatogram building was limited to peaks greater than 0.1 min with a tolerance of 0.05  $m/z$  and a minimum height of 1e3. Data smoothing was performed at a filter width of 5. Chromatogram deconvolution was performed by utilizing a local minimum search with a chromatographic threshold of 95%, a minimum relative height of 10%, a minimum absolute height of 3e3, a minimum ratio of peak to edge of 1, and a peak duration range of 0.1 to 5.0 min. The spectra were de-isotoped with a 1-ppm  $m/z$  tolerance before all treatments were aligned, and duplicate peaks were combined with a tolerance of 0.1  $m/z$  and a 3.0-min RT. Peak finder gap filling was performed with 50% intensity tolerance and 0.1  $m/z$  tolerance. Peak lists were

exported to Metaboanalyst (85), where missing values were replaced with half the minimum positive value, data were filtered by the interquartile range, and log transformation of the data was employed.

**Data availability.** All RNA-seq and ChIP-seq data files are available from the NCBI Gene Expression Omnibus database (*wetA* RNA-seq, accession number [GSE114143](https://doi.org/10.1101/14143); *vosA* and *velB* RNA-seq, accession number [GSE154639](https://doi.org/10.1101/154639); *WetA* ChIP-seq, accession number [GSE114141](https://doi.org/10.1101/141414); *VosA* and *VelB* ChIP-seq, accession number [GSE154630](https://doi.org/10.1101/154630)).

## SUPPLEMENTAL MATERIAL

Supplemental material is available online only.

**FIG S1**, TIF file, 0.5 MB.

**FIG S2**, TIF file, 0.5 MB.

**FIG S3**, TIF file, 0.3 MB.

**TABLE S1**, XLSX file, 0.02 MB.

**TABLE S2**, XLSX file, 0.02 MB.

**TABLE S3**, XLSX file, 0.1 MB.

**TABLE S4**, XLSX file, 0.01 MB.

**TABLE S5**, XLSX file, 0.02 MB.

**TABLE S6**, XLSX file, 0.02 MB.

**TABLE S7**, XLSX file, 0.04 MB.

## ACKNOWLEDGMENTS

The work at UW-Madison was supported by the National Institute of Food and Agriculture, U.S. Department of Agriculture, Hatch project 1009695 (M.-Y.W. and H.M.), and by the University of Wisconsin—Madison Office of the Vice Chancellor for Research and Graduate Education (OVCERGE) with funding from the Wisconsin Alumni Research Foundation to J.-H.Y. The work by K.-H.H. was supported by the Intelligent Synthetic Biology Center of Global Frontier Projects (2015M3A6A8065838) and by the Basic Science Research Program through the National Research Foundation of Korea (NRF) (NRF-2017R1D1A3B06035312) funded by the South Korean government. The work by H.-S.P. was supported by NRF grants to H.-S.P. funded by the South Korean government (NRF-2016R1C1B2010945 and NRF-2020R1C1C1004473). The work by M.-K.L. was supported by the KRIBB Research Initiative Program (KGM5232022). The work by G.F.N., D.A.A., and S.L. was supported by U.S. National Science Foundation grant CH-1808717. The work by A.R. and M.E.M. was supported by National Science Foundation grant DEB-1442113 and a discovery grant from Vanderbilt University.

## REFERENCES

1. Ebbole DJ. 2010. The conidium, p 577–590. In Borkovich KA, Ebbole DJ (ed), Cellular and molecular biology of filamentous fungi. ASM Press, Washington, DC.
2. Wyatt TT, Wosten HA, Dijksterhuis J. 2013. Fungal spores for dispersion in space and time. *Adv Appl Microbiol* 85:43–91. <https://doi.org/10.1016/B978-0-12-407672-3.00002-2>.
3. Park JH, Ryu SH, Lee JY, Kim HJ, Kwak SH, Jung J, Lee J, Sung H, Kim S-H. 2019. Airborne fungal spores and invasive aspergillosis in hematologic units in a tertiary hospital during construction: a prospective cohort study. *Antimicrob Resist Infect Control* 8:88. <https://doi.org/10.1186/s13756-019-0543-1>.
4. Latgé J-P. 1999. *Aspergillus fumigatus* and aspergillosis. *Clin Microbiol Rev* 12:310–350. <https://doi.org/10.1128/CMR.12.2.310>.
5. Park H-S, Yu J-H. 2012. Genetic control of asexual sporulation in filamentous fungi. *Curr Opin Microbiol* 15:669–677. <https://doi.org/10.1016/j.mib.2012.09.006>.
6. Ojeda-Lopez M, Chen W, Eagle CE, Gutierrez G, Jia WL, Swilaiman SS, Huang Z, Park HS, Yu JH, Canovas D, Dyer PS. 2018. Evolution of asexual and sexual reproduction in the aspergilli. *Stud Mycol* 91:37–59. <https://doi.org/10.1016/j.simyco.2018.10.002>.
7. Casselton L, Zolan M. 2002. The art and design of genetic screens: filamentous fungi. *Nat Rev Genet* 3:683–697. <https://doi.org/10.1038/nrg889>.
8. Martinelli SD. 1994. *Aspergillus nidulans* as an experimental organism. *Prog Ind Microbiol* 29:33–58.
9. Adams TH, Wieser JK, Yu J-H. 1998. Asexual sporulation in *Aspergillus nidulans*. *Microbiol Mol Biol Rev* 62:35–54. <https://doi.org/10.1128/MMBR.62.1.35-54.1998>.
10. Etxebeste O, Espeso EA. 2020. *Aspergillus nidulans* in the post-genomic era: a top-model filamentous fungus for the study of signaling and homeostasis mechanisms. *Int Microbiol* 23:5–22. <https://doi.org/10.1007/s10123-019-00064-6>.
11. Park H-S, Yu J-H. 2016. Molecular biology of asexual sporulation in filamentous fungi, p 3–20. In Hoffmeister D (ed), *The Mycota: a comprehensive treatise on fungi as experimental systems for basic and applied research*. Biochemistry and molecular biology, book 3, 3rd ed. Springer, Cham, Switzerland.
12. de Vries RP, Riley R, Wiebenga A, Aguilar-Osorio G, Amillis S, Uchima CA, Anderluh G, Asadollahi M, Askin M, Barry K, Battaglia E, Bayram O, Benocci T, Braus-Stromeyer SA, Caldana C, Canovas D, Cerqueira GC, Chen FS, Chen WP, Choi C, Clum A, dos Santos RAC, Damasio ARDL, Diallina G, Emri T, Fekete E, Flipphi M, Freyberg S, Gallo A, Gournas C, Habgood R, Hainaut M, Harispe ML, Henrissat B, Hilden KS, Hope R, Hossain A, Karabika E, Karaffa L, Karanyi Z, Krasevec N, Kuo A, Kusch H, LaButti K, Lagendijk EL, Lapidus A, Levasseur A, Lindquist E, Lipzen A, Logrieco AF, et al. 2017. Comparative genomics reveals high biological diversity and specific adaptations in the industrially and medically important fungal genus *Aspergillus*. *Genome Biol* 18:28. <https://doi.org/10.1186/s13059-017-1151-0>.
13. Etxebeste O, Garzia A, Espeso EA, Ugalde U. 2010. *Aspergillus nidulans*

- asexual development: making the most of cellular modules. *Trends Microbiol* 18:569–576. <https://doi.org/10.1016/j.tim.2010.09.007>.
14. Seo JA, Guan Y, Yu JH. 2006. FluG-dependent asexual development in *Aspergillus nidulans* occurs via derepression. *Genetics* 172:1535–1544. <https://doi.org/10.1534/genetics.105.052258>.
  15. Lee MK, Kwon NJ, Lee IS, Jung S, Kim SC, Yu JH. 2016. Negative regulation and developmental competence in *Aspergillus*. *Sci Rep* 6:28874. <https://doi.org/10.1038/srep28874>.
  16. Lee MK, Kwon NJ, Choi JM, Lee IS, Jung S, Yu JH. 2014. NsdD is a key repressor of asexual development in *Aspergillus nidulans*. *Genetics* 197:159–173. <https://doi.org/10.1534/genetics.114.161430>.
  17. Timberlake WE. 1990. Molecular genetics of *Aspergillus* development. *Annu Rev Genet* 24:5–36. <https://doi.org/10.1146/annurev.ge.24.120190.000253>.
  18. Mirabito PM, Adams TH, Timberlake WE. 1989. Interactions of three sequentially expressed genes control temporal and spatial specificity in *Aspergillus* development. *Cell* 57:859–868. [https://doi.org/10.1016/0092-8674\(89\)90800-3](https://doi.org/10.1016/0092-8674(89)90800-3).
  19. Adams TH, Boylan MT, Timberlake WE. 1988. *brlA* is necessary and sufficient to direct conidiophore development in *Aspergillus nidulans*. *Cell* 54:353–362. [https://doi.org/10.1016/0092-8674\(88\)90198-5](https://doi.org/10.1016/0092-8674(88)90198-5).
  20. Adams TH, Deising H, Timberlake WE. 1990. *brlA* requires both zinc fingers to induce development. *Mol Cell Biol* 10:1815–1817. <https://doi.org/10.1128/mcb.10.4.1815>.
  21. Andrianopoulos A, Timberlake WE. 1991. ATTS, a new and conserved DNA binding domain. *Plant Cell* 3:747–748. <https://doi.org/10.1105/tpc.3.8.747>.
  22. Andrianopoulos A, Timberlake WE. 1994. The *Aspergillus nidulans abaA* gene encodes a transcriptional activator that acts as a genetic switch to control development. *Mol Cell Biol* 14:2503–2515. <https://doi.org/10.1128/mcb.14.4.2503>.
  23. Sewall TC, Mims CW, Timberlake WE. 1990. *abaA* controls phialide differentiation in *Aspergillus nidulans*. *Plant Cell* 2:731–739. <https://doi.org/10.1105/tpc.2.8.731>.
  24. Sewall TC, Mims CW, Timberlake WE. 1990. Conidium differentiation in *Aspergillus nidulans* wild-type and wet-white (*wetA*) mutant strains. *Dev Biol* 138:499–508. [https://doi.org/10.1016/0012-1606\(90\)90215-5](https://doi.org/10.1016/0012-1606(90)90215-5).
  25. Wu M-Y, Mead ME, Lee M-K, Ostrem Loss EM, Kim S-C, Rokas A, Yu J-H. 2018. Systematic dissection of the evolutionarily conserved WetA developmental regulator across a genus of filamentous fungi. *mBio* 9:e01130-18. <https://doi.org/10.1128/mBio.01130-18>.
  26. Marshall MA, Timberlake WE. 1991. *Aspergillus nidulans wetA* activates spore-specific gene expression. *Mol Cell Biol* 11:55–62. <https://doi.org/10.1128/mcb.11.1.55>.
  27. Park HS, Ni M, Jeong KC, Kim YH, Yu JH. 2012. The role, interaction and regulation of the velvet regulator VelB in *Aspergillus nidulans*. *PLoS One* 7:e45935. <https://doi.org/10.1371/journal.pone.0045935>.
  28. Ni M, Yu JH. 2007. A novel regulator couples sporogenesis and trehalose biogenesis in *Aspergillus nidulans*. *PLoS One* 2:e970. <https://doi.org/10.1371/journal.pone.0000970>.
  29. Ahmed YL, Gerke J, Park H-S, Bayram O, Neumann P, Ni M, Dickmanns A, Kim SC, Yu J-H, Braus GH, Ficner R. 2013. The velvet family of fungal regulators contains a DNA-binding domain structurally similar to NF-kappaB. *PLoS Biol* 11:e1001750. <https://doi.org/10.1371/journal.pbio.1001750>.
  30. Park H-S, Yu YM, Lee M-K, Maeng PJ, Kim SC, Yu J-H. 2015. Velvet-mediated repression of beta-glucan synthesis in *Aspergillus nidulans* spores. *Sci Rep* 5:10199. <https://doi.org/10.1038/srep10199>.
  31. Park H-S, Yu J-H. 2016. Velvet regulators in *Aspergillus* spp. *Microbiol Biotechnol Lett* 44:409–419. <https://doi.org/10.4014/mbl.1607.07007>.
  32. Bayram O, Braus GH. 2012. Coordination of secondary metabolism and development in fungi: the velvet family of regulatory proteins. *FEMS Microbiol Rev* 36:1–24. <https://doi.org/10.1111/j.1574-6976.2011.00285.x>.
  33. Park H-S, Nam TY, Han KH, Kim SC, Yu J-H. 2014. VelC positively controls sexual development in *Aspergillus nidulans*. *PLoS One* 9:e89883. <https://doi.org/10.1371/journal.pone.0089883>.
  34. Kim MJ, Lee MK, Pham HQ, Gu MJ, Zhu B, Son SH, Hahn D, Shin JH, Yu JH, Park HS, Han KH. 2020. The velvet regulator VosA governs survival and secondary metabolism of sexual spores in *Aspergillus nidulans*. *Genes (Basel)* 11:103. <https://doi.org/10.3390/genes11010103>.
  35. Sarikaya Bayram O, Bayram O, Valerius O, Park H-S, Irniger S, Gerke J, Ni M, Han KH, Yu J-H, Braus GH. 2010. LaeA control of velvet family regulatory proteins for light-dependent development and fungal cell-type specificity. *PLoS Genet* 6:e1001226. <https://doi.org/10.1371/journal.pgen.1001226>.
  36. Wu MY, Mead ME, Kim SC, Rokas A, Yu JH. 2017. WetA bridges cellular and chemical development in *Aspergillus flavus*. *PLoS One* 12:e0179571. <https://doi.org/10.1371/journal.pone.0179571>.
  37. Tao L, Yu JH. 2011. AbaA and WetA govern distinct stages of *Aspergillus fumigatus* development. *Microbiology (Reading)* 157:313–326. <https://doi.org/10.1099/mic.0.044271-0>.
  38. Eom TJ, Moon H, Yu JH, Park HS. 2018. Characterization of the velvet regulators in *Aspergillus flavus*. *J Microbiol* 56:893–901. <https://doi.org/10.1007/s12275-018-8417-4>.
  39. Park HS, Bayram O, Braus GH, Kim SC, Yu JH. 2012. Characterization of the velvet regulators in *Aspergillus fumigatus*. *Mol Microbiol* 86:937–953. <https://doi.org/10.1111/mmi.12032>.
  40. Bayram O, Krappmann S, Ni M, Bok JW, Helmstaedt K, Valerius O, Braus-Stromeyer S, Kwon NJ, Keller NP, Yu JH, Braus GH. 2008. VelB/VeA/LaeA complex coordinates light signal with fungal development and secondary metabolism. *Science* 320:1504–1506. <https://doi.org/10.1126/science.1155888>.
  41. Yu J, Chang PK, Ehrlich KC, Cary JW, Bhatnagar D, Cleveland TE, Payne GA, Linz JE, Woloshuk CP, Bennett JW. 2004. Clustered pathway genes in aflatoxin biosynthesis. *Appl Environ Microbiol* 70:1253–1262. <https://doi.org/10.1128/aem.70.3.1253-1262.2004>.
  42. Brown DW, Yu JH, Kelkar HS, Fernandes M, Nesbitt TC, Keller NP, Adams TH, Leonard TJ. 1996. Twenty-five coregulated transcripts define a sterigmatocystin gene cluster in *Aspergillus nidulans*. *Proc Natl Acad Sci U S A* 93:1418–1422. <https://doi.org/10.1073/pnas.93.4.1418>.
  43. Chiang YM, Szweczyk E, Nayak T, Davidson AD, Sanchez JF, Lo HC, Ho WY, Simityan H, Kuo E, Praseuth A, Watanabe K, Oakley BR, Wang CC. 2008. Molecular genetic mining of the *Aspergillus* secondary metabolome: discovery of the emericellamide biosynthetic pathway. *Chem Biol* 15:527–532. <https://doi.org/10.1016/j.chembiol.2008.05.010>.
  44. Oh DC, Kauffman CA, Jensen PR, Fenical W. 2007. Induced production of emericellamides A and B from the marine-derived fungus *Emericella* sp. in competing co-culture. *J Nat Prod* 70:515–520. <https://doi.org/10.1021/np060381f>.
  45. Lo HC, Entwistle R, Guo CJ, Ahuja M, Szweczyk E, Hung JH, Chiang YM, Oakley BR, Wang CC. 2012. Two separate gene clusters encode the biosynthetic pathway for the meroterpenoids austinol and dehydroaustinol in *Aspergillus nidulans*. *J Am Chem Soc* 134:4709–4720. <https://doi.org/10.1021/ja209809t>.
  46. Yu JH, Wieser J, Adams TH. 1996. The *Aspergillus* FlbA RGS domain protein antagonizes G protein signaling to block proliferation and allow development. *EMBO J* 15:5184–5190. <https://doi.org/10.1002/j.1460-2075.1996.tb00903.x>.
  47. Kwon NJ, Garzia A, Espeso EA, Ugalde U, Yu JH. 2010. FlbC is a putative nuclear C<sub>2</sub>H<sub>2</sub> transcription factor regulating development in *Aspergillus nidulans*. *Mol Microbiol* 77:1203–1219. <https://doi.org/10.1111/j.1365-2958.2010.02782.x>.
  48. Kim HR, Chae KS, Han KH, Han DM. 2009. The *nsdC* gene encoding a putative C<sub>2</sub>H<sub>2</sub>-type transcription factor is a key activator of sexual development in *Aspergillus nidulans*. *Genetics* 182:771–783. <https://doi.org/10.1534/genetics.109.101667>.
  49. Vienken K, Fischer R. 2006. The Zn(II)2Cys6 putative transcription factor NosA controls fruiting body formation in *Aspergillus nidulans*. *Mol Microbiol* 61:544–554. <https://doi.org/10.1111/j.1365-2958.2006.05257.x>.
  50. Jun SC, Lee SJ, Park HJ, Kang JY, Leem YE, Yang TH, Chang MH, Kim JM, Jang SH, Kim HG, Han DM, Chae KS, Jahng KY. 2011. The MpkB MAP kinase plays a role in post-karyogamy processes as well as in hyphal anastomosis during sexual development in *Aspergillus nidulans*. *J Microbiol* 49:418–430. <https://doi.org/10.1007/s12275-011-0193-3>.
  51. Park HS, Lee MK, Kim SC, Yu JH. 2017. The role of VosA/VelB-activated developmental gene *vadA* in *Aspergillus nidulans*. *PLoS One* 12:e0177099. <https://doi.org/10.1371/journal.pone.0177099>.
  52. Navarro RE, Stringer MA, Hansberg W, Timberlake WE, Aguirre J. 1996. *catA*, a new *Aspergillus nidulans* gene encoding a developmentally regulated catalase. *Curr Genet* 29:352–359.
  53. Mayorga ME, Timberlake WE. 1992. The developmentally regulated *Aspergillus nidulans wa* gene encodes a polypeptide homologous to polyketide and fatty acid synthases. *Mol Gen Genet* 235:205–212. <https://doi.org/10.1007/BF00279362>.
  54. Suzuki S, Sarikaya Bayram O, Bayram O, Braus GH. 2013. *conF* and *conJ* contribute to conidia germination and stress response in the filamentous fungus *Aspergillus nidulans*. *Fungal Genet Biol* 56:42–53. <https://doi.org/10.1016/j.fgb.2013.04.008>.
  55. Belaish R, Sharon H, Levdansky E, Greenstein S, Shadkhan Y, Osheroov N. 2008. The *Aspergillus nidulans ceta* and *cala* genes are involved in conidia

- germination and cell wall morphogenesis. *Fungal Genet Biol* 45:232–242. <https://doi.org/10.1016/j.fgb.2007.07.005>.
56. Oshero N, Mathew J, Romans A, May GS. 2002. Identification of conidial-enriched transcripts in *Aspergillus nidulans* using suppression subtractive hybridization. *Fungal Genet Biol* 37:197–204. [https://doi.org/10.1016/S1087-1845\(02\)00502-9](https://doi.org/10.1016/S1087-1845(02)00502-9).
  57. Sewall TC. 1994. Cellular effects of misscheduled *brlA*, *abaA*, and *wetA* expression in *Aspergillus nidulans*. *Can J Microbiol* 40:1035–1042. <https://doi.org/10.1139/m94-164>.
  58. Son Y-E, Park H-S. 2020. Genome wide analysis reveals the role of *VadA* in stress response, germination, and sterigmatocystin production in *Aspergillus nidulans* conidia. *Microorganisms* 8:1319. <https://doi.org/10.3390/microorganisms8091319>.
  59. Baltussen TJH, Zoll J, Verweij PE, Melchers WJG. 2020. Molecular mechanisms of conidial germination in *Aspergillus* spp. *Microbiol Mol Biol Rev* 84:e00049-19. <https://doi.org/10.1128/MMBR.00049-19>.
  60. Thammahong A, Puttikamonkul S, Perfect JR, Brennan RG, Cramer RA. 2017. Central role of the trehalose biosynthesis pathway in the pathogenesis of human fungal infections: opportunities and challenges for therapeutic development. *Microbiol Mol Biol Rev* 81:e00053-16. <https://doi.org/10.1128/MMBR.00053-16>.
  61. Lara-Rojas F, Sanchez O, Kawasaki L, Aguirre J. 2011. *Aspergillus nidulans* transcription factor *AtfA* interacts with the MAPK *SakA* to regulate general stress responses, development and spore functions. *Mol Microbiol* 80:436–454. <https://doi.org/10.1111/j.1365-2958.2011.07581.x>.
  62. Sakamoto K, Arima TH, Iwashita K, Yamada O, Gomi K, Akita O. 2008. *Aspergillus oryzae atfB* encodes a transcription factor required for stress tolerance in conidia. *Fungal Genet Biol* 45:922–932. <https://doi.org/10.1016/j.fgb.2008.03.009>.
  63. Han KH, Prade RA. 2002. Osmotic stress-coupled maintenance of polar growth in *Aspergillus nidulans*. *Mol Microbiol* 43:1065–1078. <https://doi.org/10.1046/j.1365-2958.2002.02774.x>.
  64. Bayram O, Feussner K, Dumkow M, Herrfurth C, Feussner I, Braus GH. 2016. Changes of global gene expression and secondary metabolite accumulation during light-dependent *Aspergillus nidulans* development. *Fungal Genet Biol* 87:30–53. <https://doi.org/10.1016/j.fgb.2016.01.004>.
  65. Kafer E. 1977. Meiotic and mitotic recombination in *Aspergillus* and its chromosomal aberrations. *Adv Genet* 19:33–131. [https://doi.org/10.1016/S0065-2660\(08\)60245-x](https://doi.org/10.1016/S0065-2660(08)60245-x).
  66. Kim D, Perteza G, Trapnell C, Pimentel H, Kelley R, Salzberg SL. 2013. TopHat2: accurate alignment of transcriptomes in the presence of insertions, deletions and gene fusions. *Genome Biol* 14:R36. <https://doi.org/10.1186/gb-2013-14-4-r36>.
  67. Anders S, Pyl PT, Huber W. 2015. HTSeq—a Python framework to work with high-throughput sequencing data. *Bioinformatics* 31:166–169. <https://doi.org/10.1093/bioinformatics/btu638>.
  68. Love MI, Huber W, Anders S. 2014. Moderated estimation of fold change and dispersion for RNA-seq data with DESeq2. *Genome Biol* 15:550. <https://doi.org/10.1186/s13059-014-0550-8>.
  69. Bolger AM, Lohse M, Usadel B. 2014. Trimmomatic: a flexible trimmer for Illumina sequence data. *Bioinformatics* 30:2114–2120. <https://doi.org/10.1093/bioinformatics/btu170>.
  70. Li H. 2013. Aligning sequence reads, clone sequences and assembly contigs with BWA-MEM. *arXiv* 1303.3997. <https://arxiv.org/abs/1303.3997>.
  71. Li H, Handsaker B, Wysoker A, Fennell T, Ruan J, Homer N, Marth G, Abecasis G, Durbin R, 1000 Genome Project Data Processing Subgroup. 2009. The Sequence Alignment/Map format and SAMtools. *Bioinformatics* 25:2078–2079. <https://doi.org/10.1093/bioinformatics/btp352>.
  72. Landt SG, Marinov GK, Kundaje A, Kheradpour P, Pauli F, Batzoglou S, Bernstein BE, Bickel P, Brown JB, Cayting P, Chen Y, DeSalvo G, Epstein C, Fisher-Aylor KI, Euskirchen G, Gerstein M, Gertz J, Hartemink AJ, Hoffman MM, Iyer VR, Jung YL, Karmakar S, Kellis M, Kharchenko PV, Li Q, Liu T, Liu XS, Ma L, Milosavljevic A, Myers RM, Park PJ, Pazin MJ, Perry MD, Raha D, Reddy TE, Rozowsky J, Shores N, Sidow A, Slattery M, Stamatoyannopoulos JA, Tolstorukov MY, White KP, Xi S, Farnham PJ, Lieb JD, Wold BJ, Snyder M. 2012. ChIP-seq guidelines and practices of the ENCODE and modENCODE consortia. *Genome Res* 22:1813–1831. <https://doi.org/10.1101/gr.136184.111>.
  73. Kharchenko PV, Tolstorukov MY, Park PJ. 2008. Design and analysis of ChIP-seq experiments for DNA-binding proteins. *Nat Biotechnol* 26:1351–1359. <https://doi.org/10.1038/nbt.1508>.
  74. Zhang Y, Liu T, Meyer CA, Eeckhoute J, Johnson DS, Bernstein BE, Nusbaum C, Myers RM, Brown M, Li W, Liu XS. 2008. Model-based analysis of ChIP-Seq (MACS). *Genome Biol* 9:R137. <https://doi.org/10.1186/gb-2008-9-9-r137>.
  75. Machanick P, Bailey TL. 2011. MEME-ChIP: motif analysis of large DNA datasets. *Bioinformatics* 27:1696–1697. <https://doi.org/10.1093/bioinformatics/btr189>.
  76. Arnaud MB, Chibucos MC, Costanzo MC, Crabtree J, Inglis DO, Lotia A, Orvis J, Shah P, Skrzypek MS, Binkley G, Miyasato SR, Wortman JR, Sherlock G. 2010. The *Aspergillus* Genome Database, a curated comparative genomics resource for gene, protein and sequence information for the *Aspergillus* research community. *Nucleic Acids Res* 38:D420–D427. <https://doi.org/10.1093/nar/gkp751>.
  77. Stajich JE, Harris T, Brunk BP, Brestelli J, Fischer S, Harb OS, Kissinger JC, Li W, Nayak V, Pinney DF, Stoeckert CJ, Jr, Roos DS. 2012. FungiDB: an integrated functional genomics database for fungi. *Nucleic Acids Res* 40:D675–D681. <https://doi.org/10.1093/nar/gkr918>.
  78. Ge SX, Jung D, Yao R. 2020. ShinyGO: a graphical enrichment tool for animals and plants. *Bioinformatics* 36:2628–2629. <https://doi.org/10.1093/bioinformatics/btz931>.
  79. Wang PM, Choera T, Wiemann P, Pisithkul T, Amador-Noguez D, Keller NP. 2016. TrpE feedback mutants reveal roadblocks and conduits toward increasing secondary metabolism in *Aspergillus fumigatus*. *Fungal Genet Biol* 89:102–113. <https://doi.org/10.1016/j.fgb.2015.12.002>.
  80. Ostrem Loss EM, Lee M-K, Wu M-Y, Martien J, Chen W, Amador-Noguez D, Jefcoate C, Remucal C, Jung S, Kim S-C, Yu J-H. 2019. Cytochrome P450 monooxygenase-mediated metabolic utilization of benzo[a]pyrene by *Aspergillus* species. *mBio* 10:e00558-19. <https://doi.org/10.1128/mBio.00558-19>.
  81. Adpressa DA, Stalheim KJ, Proteau PJ, Loesgen S. 2017. Unexpected bio-transformation of the HDAC inhibitor vorinostat yields aniline-containing fungal metabolites. *ACS Chem Biol* 12:1842–1847. <https://doi.org/10.1021/acschembio.7b00268>.
  82. Adpressa DA, Connolly LR, Konkel ZM, Neuhaus GF, Chang XL, Pierce BR, Smith KM, Freitag M, Loesgen S. 2019. A metabolomics-guided approach to discover *Fusarium graminearum* metabolites after removal of a repressive histone modification. *Fungal Genet Biol* 132:103256. <https://doi.org/10.1016/j.fgb.2019.103256>.
  83. Pluskal T, Castillo S, Villar-Briones A, Oresic M. 2010. MZmine 2: modular framework for processing, visualizing, and analyzing mass spectrometry-based molecular profile data. *BMC Bioinformatics* 11:395. <https://doi.org/10.1186/1471-2105-11-395>.
  84. Abdelmohsen UR, Cheng C, Viegmann C, Zhang T, Grkovic T, Ahmed S, Quinn RJ, Hentschel U, Edrada-Ebel R. 2014. Dereplication strategies for targeted isolation of new antitrypanosomal actinosporins A and B from a marine sponge associated-*Actinokineospora* sp. EG49. *Mar Drugs* 12:1220–1244. <https://doi.org/10.3390/md12031220>.
  85. Xia J, Sinelnikov IV, Han B, Wishart DS. 2015. MetaboAnalyst 3.0—making metabolomics more meaningful. *Nucleic Acids Res* 43:W251–W257. <https://doi.org/10.1093/nar/gkv380>.